Tellus B
Chemical and Physical Meteorology

Evaluation of Data Processing Strategies for Methane Isotopic Signatures Determined During Near-Source Measurements

ORIGINAL RESEARCH PAPER

SARA M. DEFRATYKA
JAMES L. FRANCE
REBECCA E. FISHER
DAVE LOWRY
JULIANNE M. FERNANDEZ
SEMRA BAKKALOGLU
CAMILLE YVER-KWOK
JEAN-DANIEL PARIS
PHILIPPE BOUSQUET
TIM ARNOLD
CHRIS RENNICK
JON HELMORE
NIGEL YARROW
EUAN G. NISBET

*Author affiliations can be found in the back matter of this article

STOCKHOLM UNIVERSITY PRESS

ABSTRACT

Mobile, near-source measurements are broadly used for determining $\delta^{13}CH_4$ of individual methane (CH_4) emissions sources. To answer the need for robust and comparable measurement methods, we aim to define the best practices to determine isotopic signatures of CH_4 sources from atmospheric measurements, considering instrument accuracy and precision. Using the Keeling and Miller-Tans methods, we verify the impact of linear fitting methods, averaging approaches, and for the Miller-Tans method, different background composition. Measurement techniques include Isotope Ratio Mass Spectrometry (IRMS) and Cavity Ring Down Spectroscopy (CRDS). The use of the active AirCore system for sampling, coupled to CRDS for measurement, is examined. Due to their higher precision and accuracy, the chosen data processing strategy does not significantly influence IRMS results. Comparatively lower-precision CRDS measurements are more sensitive to methodological choices. Fitting methods with forced symmetry like Major Axis or Bivariate Correlated Errors and Intrinsic Scatter (BCES) with orthogonal sub-method introduce significant bias in the determined $\delta^{13}CH_4$ signatures using measurements from the lower-precision CRDS. The most reliable results are obtained for non-averaged data using fitting methods, which include uncertainties of x- and y-axis values, like York fitting or BCES (Y|X) sub-method, where x is treated as an independent variable. The Ordinary Least Squares method provides sufficiently robust results and can be used to determine $\delta^{13}CH_4$ in near-source conditions. The present recommendations are aimed at laboratories measuring $\delta^{13}CH_4$ source signatures to encourage consistency in the required methods for data analysis.

CORRESPONDING AUTHOR:
Sara M. Defratyka
School of GeoSciences, University of Edinburgh, Edinburgh, UK; National Physical Laboratory, Hampton Road, Teddington, UK
sara.defratyka@ed.ac.uk

KEYWORDS:
CH_4; Keeling plot; Miller-Tans plot; isotopic signature

TO CITE THIS ARTICLE:
Defratyka, S.M., France, J.L., Fisher, R.E., Lowry, D., Fernandez, J.M., Bakkaloglu, S., Yver-Kwok, C., Paris, J.-D., Bousquet, P., Arnold, T., Rennick, C., Helmore, J., Yarrow, N. and Nisbet, E.G. 2025. Evaluation of Data Processing Strategies for Methane Isotopic Signatures Determined During Near-Source Measurements. *Tellus B: Chemical and Physical Meteorology*, 77(1): 1–17. DOI: https://doi.org/10.16993/tellusb.1878

1. INTRODUCTION

Tracers, such as alkanes (e.g., ethane) or stable isotope ratios, measured alongside the CH_4 mole fraction, provide additional information to determine sources of emissions (Basu et al., 2022; Germain-Piaulenne et al., 2024; Rella et al., 2015; Sherwood et al., 2017; Simpson et al., 2012; Turner et al., 2019). Typically, stable carbon isotopic signatures of methane emissions (expressed as $\delta^{13}CH_4$) are widely used, from local to global scales to identify biogenic, thermogenic, and pyrogenic emission sources and to better constrain CH_4 budget changes (e.g., Al-Shalan et al., 2022; Defratyka et al., 2021; Hoheisel et al., 2019; Lopez et al., 2017; Maazallahi et al., 2020; Menoud et al., 2021, 2020; Phillips et al., 2013; Rella et al., 2015; Röckmann et al., 2016).

However, beyond the biogenic/thermogenic separation, $\delta^{13}CH_4$ values of an individual methane emitter from any sector (e.g., landfill, natural gas compressor) can vary widely, depending on numerous factors, such as the CH_4 formation process, location, or management practice (e.g., Chanton et al., 2000; Menoud et al., 2022; Sherwood et al., 2017; Whiticar, 1999). Moreover, $\delta^{13}CH_4$ signatures for some sectors are spread across a wide range and overlap with $\delta^{13}CH_4$ for other sectors (e.g., Bakkaloglu et al., 2022; Fernandez et al., 2022; Menoud et al., 2022; Sherwood et al., 2017). Therefore, a better characterization of $\delta^{13}CH_4$ source signatures can improve their source attribution in top-down emission studies (atmospheric observation combined with the inverse modeling), (e.g., Saunois et al., 2020; Varga et al. 2021; Basu et al. 2022). It can also verify bottom-up quantitative approaches, based on process-based models, inventories, and data extrapolation (Lan et al., 2021; Rigby et al., 2012; Schwietzke et al., 2016).

$\delta^{13}CH_4$ can be measured for emission plumes downwind of sources from individual sectors (e.g., natural gas, agriculture, landfill) by taking bag/canister samples followed by later measurement in the laboratory (e.g., Bakkaloglu et al. 2021; 2022; Lowry et al. 2020; Townsend-Small et al. 2012; 2016). An alternative is to deploy in-situ instruments, for example, Cavity Ring Down Spectroscopy (CRDS) systems. Such analyser can be equipped with an atmospheric sampling system, called AirCore (air storage tool) (Karion et al., 2010; Rella et al., 2015), to increase number of datapoint, what improves measurements' precision (Defratyka et al., 2021; Hoheisel et al., 2019; Lopez et al., 2017). Calculating the $\delta^{13}CH_4$ source signature (subsequently referred to as $\delta^{13}CH_{4\ source}$) is complicated by mixing between source emissions and 'background' air, i.e., the atmospheric air remote from any source.

To extract the $\delta^{13}CH_{4\ source}$ from ambient air samples downwind of a source, Keeling or Miller-Tans methods can be used (Keeling, 1961; Miller and Tans, 2003; Pataki et al., 2003). These methods are based on the principle of mass balance conservation. Both methods use a linear regression to determine $\delta^{13}CH_4$ source. As such, the calculation method of choice has an impact on determining a source's isotopic signature and can potentially bias the determined $\delta^{13}CH_4$ source (Miller and Tans 2003; Wehr and Saleska 2017; Zobitz et al. 2006).

Previously, the verification of Keeling and Miller-Tans methods and application of different linear fitting methods was made mostly using synthetic data and theoretical calculation (Wehr and Saleska, 2017; Zobitz et al., 2006) or larger dataset of CO_2 respiration (Miller and Tans, 2003; Pataki et al., 2003). Hoheisel et al. (2019) provided a comparison of $\delta^{13}CH_{4\ source}$ calculated from atmospheric measurements and synthetic data. However, they focused only on the comparison of two linear fitting methods: Ordinary Least Squares method and York fitting. Here, we analyze data from atmospheric, near-source measurements under controlled but realistic field conditions, and include consideration of measurement frequency and instrument uncertainty. Until now, different laboratories use various analytical strategies (e.g. Defratyka et al., 2021; Fernandez et al., 2022; Hoheisel et al., 2019; Lopez et al., 2017; Menoud et al., 2022), that may affect the reported $\delta^{13}CH_{4\ source}$ and impede inter-laboratory comparison (Menoud et al., 2022; Zobitz et al., 2006).

We analyze isotopic measurement and samples collected within a controlled release experiment to derive a more universal analytical approach for near-source studies of $\delta^{13}CH_{4\ source}$. The controlled release experiment aims to be representative of real-life conditions under which existing methane sources, like natural gas infrastructure or sewage emission, are measured. The experiment focused on the validation of several methods for mobile, vehicle-based methane measurements (e.g., Defratyka et al., 2021; Fernandez et al., 2022; Hoheisel et al., 2019; Menoud et al., 2022). Samples collected over five consecutive days of the experiment were analyzed using Isotope Ratio Mass Spectrometry (IRMS) and Cavity Ring Down Spectroscopy (CRDS) measurement techniques (Sect. 2.2), while the CRDS instrument was used both for in-situ sampling using an AirCore tool, and for remote bag analysis after the sample collection. Comparing these three types of measurement techniques, we investigated 1) the influence of the analytical measurement method (IRMS or CRDS), and 2) the impact of increasing measurement frequency for the less precise CRDS. We provide an intercomparison of 1) Keeling and Miller-Tans methods (Sect. 3.1), 2) the impact of chosen backgrounds for Miller-Tans method (Sect. 3.2) and 3) the impact of averaging clusters (Sect. 3.3). Finally, data were re-analyzed using different linear fitting methods (Sect. 3.4).

2. EXPERIMENTAL SET-UP

2.1. CONTROLLED RELEASE SET UP

The controlled release experiment allows an evaluation of the accuracy and precision of mobile near-source measurements of CH_4 emission rates, ethane to methane ratios and $\delta^{13}CH_4$. Our experiment took place over 5 days in September 2019 at Bedford Aerodrome, UK. Pure methane was released from a manifolded multi-cylinder pack of twelve cylinders containing 999.6 ± 10.0 mmol mol^{-1} methane, with an initial pressure of about 200 bars. The impurities in the cylinders came from ethane (48 ± 10 µmol mol^{-1}) and propane (0.149 ± 0.30 µmol mol^{-1}). All 12 cylinders were filled at the same time from the same CH_4 source, ensuring $\delta^{13}CH_{4\ source}$ remained stable over the entire measurement period. The methane release rate varied from 25 L min^{-1} to 70 L min^{-1}. During the release, CH_4 was mixed with ethane (C_2H_6) in a varying ratio, giving C_2H_6:CH_4 ratios from 0.00 to 0.07. The purity of the C_2H_6 was 999.9 ± 10.0 mmol mol^{-1}, with impurities mostly from methane (2.27 ± 0.46 µmol mol^{-1}) and propane (7.5 ± 1.5 µmol mol^{-1}). To reach the required CH_4 emission rate, CH_4 was released simultaneously from all 12 cylinders, using a transportable flow control system (details in Gardiner et al., 2017). Briefly, the flow control system is designed and configured for the creation of 'real-life' gaseous emission scenarios, in a range of industrial settings. It allows for validation of methods for emission monitoring applied during typical field conditions. The control system is built on six mass flow controllers (MFC), (Brooks Instrument, Hatfield, PA, USA). Four primary MFCs provide independent emission sources, while two secondary MFCs allow for the introduction of purge and interferant gases into the primary flow. The flow control system is computer operated, allowing for the implementation of pre-written operational programs and the post-test analysis (Gardiner et al., 2017).

Here, the controlled release experiment involved 26 releases, each lasting about 45 minutes. The number of releases per day varied between 2 and 8. The smallest number of releases was conducted during day 1 (3 releases) and day 5 (2 releases). As well as controlling emission fluxes and the ratio of C_2H_6:CH_4, wind speed and direction were measured during all releases. Details of individual gas releases during controlled release experiment are presented in Table A1.

2.2. MEASUREMENT TECHNIQUE

During the mobile near-source measurements, the sampling method was based on driving through a plume of CH_4. Throughout each release, a vehicle intersected the multiple times plume perpendicular to the wind direction. The controlled release experiment gave the opportunity to validate the mobile laboratories of Royal Holloway, University of London (RHUL) and of the Laboratory for Sciences of Climate and Environment (LSCE). Details of evaluated mobile laboratories are presented in appendix A, with instrument characteristics in Table A2. Briefly, the RHUL mobile laboratory used for this experiment was in operation between 2013 and 2020 (Lowry et al., 2020). This vehicle was equipped with a Picarro CRDS G2301 analyzer, capable to measure mole fractions of CO_2, CH_4 and H_2O, a Los Gatos Research Ultraportable Methane Ethane Analyzer (LGR UMEA), and a manually operated diaphragm pump for filling air sample bags. Three air cylinders were measured and calibrated against the NOAA scale by the Max-Plank Institute for Biogeochemistry Jena, which were used to calibrate the Picarro CRDS G2301 before and after the measurement campaign to the WMO X2004 A CH_4 scale (Lowry et al., 2020; France et al., 2016; Zazzeri et al., 2015).

The LSCE mobile laboratory was previously used during mobile studies (e.g., Defratyka et al., 2021), and it is similar to other mobile laboratories equipped with a Picarro CRDS G2201-i (henceforth referred to as CRDS), capable of in-situ measurements of CH_4 mole fractions and $\delta^{13}CH_4$ (e.g. Rella et al. 2015; Lopez et al. 2017; Hoheisel et al. 2019). The LSCE mobile set-up also comprises of an active AirCore sampler for tripling the sampling frequency during in-situ measurements of $\delta^{13}CH_4$ (Defratyka et al., 2021). The LSCE instrument was calibrated using a 3-point mole fraction and isotopic composition calibration, just before shipping the instrument to the UK. After calibration, CH_4 mole fractions were reported on the WMO X2004 A scale and $\delta^{13}CH_4$ is reported relative to the international Vienna Pee Dee Belemnite (VPDB) standard (Craig, 1957). Due to logistical restrictions, the calibration cylinder or known working gas could not be used during the controlled release experiment. However, an additional working gas was measured in the laboratory before and after the experiment, and no significant drift was observed.

The CRDS measurements were made in a high precision mode, in CO_2-CH_4 simultaneous mode. CO_2 measurement acquisition was kept for additional trouble shooting of analytical artifacts. To resolve short temporal variabilities, the flow rate was adjusted to 100 cc min^{-1} for faster instrument response during the mobile measurements. Significant cross sensitivities between C_2H_6 and $\delta^{13}CH_4$ in the absorption spectrum have been shown to lead to biases in the measured $\delta^{13}CH_4$ by CRDS (details in Appendix A). The effect is inversely proportional to the CH_4 mole fraction and proportional to the C_2H_6 mole fraction in the sample and has been previously quantified (e.g., Rella et al. 2015; Assan et al. 2017).

2.2.1. Collected bag samples measured on IRMS

Air samples analyzed at RHUL were collected by pumping the largest observed enhancement of CH_4 plume air into 3 liter Flexfoil® bags (SKC). In total, 21 bags were collected to be measured by IRMS. During the campaign period, at least two bag samples from each CH_4 plume, plus a background sample were collected per day. These were

measured afterwards in the laboratory, using Picarro CRDS 1301 to determine CH_4 mole fraction and using continuous flow gas chromatography isotope ratio mass spectrometry (CF-GC-IRMS Isoprime mass spectrometer with Elementar Trace Gas module, henceforth called IRMS) to determine $\delta^{13}CH_4$ (Fisher et al., 2006).

2.2.2. Collected bag samples measured on CRDS

During the three initial releases (two releases over the first day, one release over the second day), bag samples were collected to be measured afterwards on the CRDS instead of using the in-situ AirCore sampler, due to a battery issue with the LSCE mobile laboratory. In total, 10 samples of ambient air were collected in 5 liter Flexfoil® bags (SKC), which allowed for about 20 minutes of measurements using the laboratory-based CRDS. After removing the initial stabilization time, around 15 minutes of measurements were analyzed. The uncertainty was estimated using the standard deviation of measured CH_4 and $\delta^{13}CH_4$ (1 standard error of 15 minutes of measurements). During this study, bag samples measured by LSCE, were collected only when CH_4 was released (C_2H_6:CH_4 = 0.00); thus, the C_2H_6 on $\delta^{13}CH_4$ correction was not applied for bag samples measured by this CRDS.

2.2.3. In-situ CRDS with AirCore

For LSCE in-situ sampling, if the largest CH_4 enhancement during the intersection of a CH_4 plume reached at least 500 nmol mol^{-1} above background, the CH_4 plume was re-sampled using the air collected and stored in the AirCore (details in Appendix A). AirCore sampling was performed during 12 of the 26 releases. For most of the releases, more than one AirCore sample was collected. In total, 31 AirCore samples were collected.

In the case of AirCore studies, $\delta^{13}CH_{4\ source}$ were determined both without applying the C_2H_6 on $\delta^{13}CH_4$ correction and with a correction.

2.2.4. Direct $\delta^{13}CH_4$ measurement of methane source

To determine $\delta^{13}CH_4$ of the source gas, a sample cylinder was filled directly from the multi-cylinder pack after the end of the experiment. Then, the sample was diluted to approximately 600 µmol mol^{-1} and measured using laser spectrometry. In the next step, 600 µmol mol^{-1} sample was diluted to 2.5 µmol mol^{-1} and measured using IRMS at RHUL (Rennick et al., 2021). $\delta^{13}CH_4$ measured by laser spectrometry is equal to –41.45 ± 0.06‰ (1 Standard Deviation – 1SD), while $\delta^{13}CH_4$ measured by IRMS reached –41.27 ± 0.06‰ (1SD) (Rennick et al., 2021). The true $\delta^{13}CH_4$ signature of the cylinder batch, defined as an average $\delta^{13}CH_4$ from both instruments, equal to –41.36 ± 0.17‰ was compared with results from samples collected using atmospheric mobile studies.

3. DATA PROCESSING AND SOURCE SIGNATURE DETERMINATION METHODS

Figure 1 presents the flow chart of steps to find the best data processing strategy for determination of $\delta^{13}CH_{4\ source}$ from near-source mobile measurements. Data collected using different measurement techniques (Sect. 2.2) are

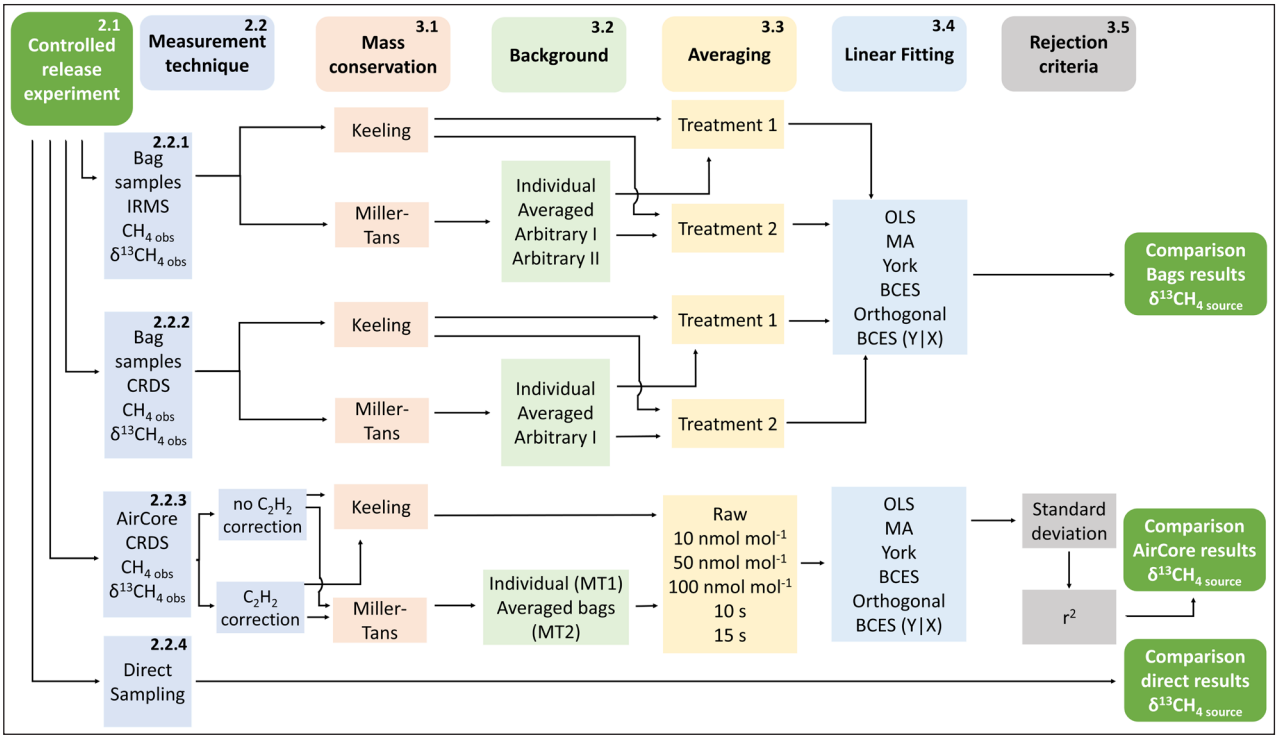

Figure 1 Flow chart of steps to find the best analytical strategy for determination of $\delta^{13}CH_4$ source signature, from mobile near-source measurements, based on controlled release experiment. The number in the top right corner corresponds to the methods subsection, where steps are explained in detail.

analyzed, both using Keeling method and Miller-Tans method (Sect. 3.1), while different backgrounds (Sect. 3.2), averaging strategies (Sect. 3.3), and linear fitting methods (Sect. 3.4) are employed.

For bag samples measured on IRMS and CRDS, determination of $\delta^{13}CH_{4\ source}$ using five regression methods (OLS, MA, York, BCES (Y|X) and BCES Orthogonal) and treatment 1 and treatment 2 averaging approach were implemented, both using Keeling method and Miller-Tans method. For Miller-Tans method, calculations are repeated using different backgrounds: local, averaged, arbitrary I and arbitrary II (Figure 1).

For each AirCore sample, six datasets of distinct clusters (raw data, 10 s, 15 s, 10 nmol mol^{-1}, 50 nmol mol^{-1} and 100 nmol mol^{-1}) were analyzed using Keeling and Miller-Tans methods. For Miller-Tans method, two different backgrounds were subtracted: individual AirCore background and averaged bag samples background. The analysis was repeated using different regression methods: OLS, MA, York, BCES (Y|X) and BCES Orthogonal (Figure 1). Additionally, the rejection criteria, based on standard deviation and r^2 values were applied for each individual AirCore (Sect. 3.5) to select which result should be kept for further analysis and comparison.

3.1. KEELING AND MILLER-TANS METHODS

During mobile near-source measurements, the observed CH_4 (hereafter $CH_{4\ obs}$) mole fraction and $\delta^{13}CH_4$ signature (hereafter $\delta^{13}CH_{4\ obs}$) are a mixture of atmospheric background CH_4 (hereafter $CH_{4\ bckg}$) and the $CH_{4\ source}$ from the source. To determine $\delta^{13}CH_{4\ source}$ the Keeling or the Miller-Tans methods can be applied (e.g. Hoheisel et al. 2019; Menoud et al., 2020; Defratyka et al., 2021; Fernandez et al., 2022). In the Keeling method (Keeling, 1961; Pataki et al., 2003), $\delta^{13}CH_{4\ obs}$ is plotted against the inverse of $CH_{4\ obs}$ mole fraction and the y-intercept of the fitted linear regression is interpreted as the $\delta^{13}CH_{4\ source}$ of the observed source:

$$\delta^{13}CH_{4obs} = CH_{4bckg} \cdot \left(\delta^{13}CH_{4bckg} - \delta^{13}CH_{4source}\right) \cdot \frac{1}{CH_{4obs}} + \delta^{13}CH_{4source} \quad (1),$$

where subscripts obs, bckg, and source refer to observed, background, and source values. Notably, parameter $CH_{4bckg} \cdot (\delta^{13}CH_{4bckg} - \delta^{13}CH_{4source})$ does not affect $\delta^{13}CH_{4\ source}$ determined as intercept of Eq. 1, and it can remain as an unknown parameter.

The Miller-Tans method (Miller and Tans, 2003) is another mass conservation approach, where the mole fraction and the isotopic signature of atmospheric background are assumed to be well known. The isotopic signature of the source is represented by the slope of a fitted linear regression, where, after background subtraction, $\delta^{13}CH_{4\ obs}$ multiplied by $CH_{4\ obs}$ mole fraction is plotted against $CH_{4\ obs}$ mole fraction:

$$\delta^{13}CH_{4obs} \cdot CH_{4obs} - \delta^{13}CH_{4bckg} \cdot CH_{4bckg} = \delta^{13}CH_{4source} \cdot (CH_{4obs} - CH_{4bckg}) \quad (2).$$

The Miller-Tans method can be useful to interpret studies, where the Keeling method assumption of stable background is unfulfilled or unknown, e.g., when studies are conducted over a long period of time (Al-Shalan et al., 2022; Lowry et al., 2020).

3.2. BACKGROUND SUBTRACTION FOR MILLER-TANS METHOD

On the small scale, the diurnal variation of CH_4 mole fraction can be observed. Additionally, some local CH_4 enhancements can exist and affect the background determination. Under these circumstances and regarding available instrumentation, one needs to decide how to define the background, which is defined as a part of the Miller-Tans method. To evaluate the impact of a chosen $CH_{4\ bckg}$ mole fraction and $\delta^{13}CH_{4\ bckg}$ isotopic signature, defined backgrounds are subtracted for the Miller-Tans method. For bag samples measured by IRMS, as a first attempt, an 'individual background' was subtracted, defined from a background bag sample collected directly after the release, when bag samples were collected within CH_4 enhancement. For example, for all bag samples collected during the first day, the background sample collected on the first day was subtracted. For the next calculation, an 'averaged background' is subtracted, which is defined as the average of all background bag samples collected over whole experiment. Next, to verify the sensitivity of Miller-Tans method for a subtracted background, calculations for two arbitrary chosen backgrounds with lower $CH_{4\ bckg}$ mole fraction and $\delta^{13}CH_{4\ bckg}$ than during the experiment were conducted: 'arbitrary I' and 'arbitrary II' background. For arbitrary I background, $CH_{4\ bckg}$ mole fraction is defined as an average global CH_4 mole fraction observed in September 2019, equal to 1.871 ± 0.001 µmol mol^{-1} (Dlugokencky, 2022), while $\delta^{13}CH_{4\ bckg}$ is defined using value from Brownlow et al., as −47.2 ± 0.2‰ (2017). For arbitrary II background, the $CH_{4\ bckg}$ mole fraction is set up the same as the arbitrary I background, but the $\delta^{13}CH_{4\ bckg}$ set to −42.7 ± 0.2 ‰.

For bag samples measured by CRDS, the Miller-Tans method is implemented three times, while defined backgrounds are subtracted. The backgrounds have been chosen similarly as for the IRMS analysis. Thus, the analysis is implemented three times where individual, averaged, and arbitrary I background are subtracted. The $CH_{4\ bckg}$ mole fraction and $\delta^{13}CH_{4\ bckg}$ for bag samples measured on IRMS and CRDS are presented in Appendix A.

In the case of in-situ AirCore sampling, for the Miller-Tans method, data were analyzed twice to examine possible impact of subtracted background. First, subtracted background is calculated individually for each AirCore, as an average of AirCore background data of an individual AirCore sample, observed directly before and after $CH_{4\ obs}$ elevation (defined for later as Miller-Tans 1). Second, averaged background of all bag samples measured on CRDS was subtracted for each individual

AirCore sample (Miller-Tans 2) to evaluate sensitivity of Miller-Tans method for subtracted background.

3.3. DATA AVERAGING

3.3.1. Data averaging bag samples measured by IRMS and CRDS

In the long-term perspective, bag samples are collected downwind of some sites during multiple visits over a few years (e.g., Lowry et al., 2020). To report $\delta^{13}CH_{4\ source}$ from multiple visits, determined $\delta^{13}CH_{4\ source}$ are averaged. Thus, in this study we verify the impact of the chosen averaging strategy on the determined $\delta^{13}CH_{4\ source}$. For bag samples under 'treatment 1,' $\delta^{13}CH_{4\ source}$ is calculated separately for each individual day and the final $\delta^{13}CH_{4\ source}$ is calculated as an average of determined $\delta^{13}CH_{4\ source}$ for individual days over five consecutive days. This approach is commonly used, however; to quantify its impact, another averaging strategy was tested. In a 'treatment 2' averaging approach, the results of bag samples from all releases are treated as one data set and $\delta^{13}CH_{4\ source}$ and its uncertainty is determined directly from the linear regression. For both treatment 1 and treatment 2 averaging approaches, different data processing strategies were implemented where individual, averaged, and arbitrary background subtraction in the Miller-Tans method were tested.

3.3.2. Data averaging AirCore in-situ sampling

For the AirCore in-situ sampling, the observed $\delta^{13}CH_{4\ obs}$ fluctuated, which can impact the determined $\delta^{13}CH_{4\ source}$. To check if data smoothing (i.e., through averaging) improves the determination of $\delta^{13}CH_{4\ source}$, observational data was averaged in clusters before being analyzed. In total, six data sets have been prepared from each AirCore sample and were further analyzed using the Keeling and Miller-Tans methods: raw data, three clusters based on CH_4 mole fraction and two time-average clusters (Figure 1). For CH_4 mole fraction clustering, clusters with steps of 10 nmol mol^{-1}, 50 nmol mol^{-1} and 100 nmol mol^{-1} were used, while for time average clusters, clusters of 10 s and 15 s time averaging were used. Examined clusters were chosen arbitrarily as a compromise between smoothing and potential bias due to over-averaging.

Typically, an individual AirCore sample's volume allows for collection of 50–80 datapoints. Similar to Hoheisel et al. (2019), AirCore sample measurement errors of individual data points are linearly interpolated based on laboratory tests (details in Appendix A). The interpolated uncertainty of individual points is used as the uncertainty for the clusters of raw data, both $CH_{4\ obs}$ mole fraction and $\delta^{13}CH_{4\ obs}$ signature, for linear fitting methods which require measurement uncertainty as an input (Section 3.4). However, when data points are clustered, based on CH_4 mole fraction or time averaging, a total uncertainty of clustered data points is a combination of both the uncertainty of clustering and uncertainty of individual, clustered points (details in Appendix A).

3.4. LINEAR FITTING METHOD

Both Keeling and Miller-Tans methods rely on linear regression fitting. Potentially, using different linear fitting methods can introduce discrepancies between determined $\delta^{13}CH_{4\ source}$ and impede its comparison (Menoud et al., 2022; Zobitz et al., 2006). Here we aim the first intercomparison of all broadly used linear regression methods to verify potential biases introduced by different linear fittings: Ordinary Least Squares (OLS) (Defratyka et al., 2021), Major Axis (MA) (Menoud et al., 2022), York fitting (Hoheisel et al., 2019) and Bivariate Correlated Errors and Intrinsic Scatter (BCES) Orthogonal (e.g., Fernandez et al., 2022), adding verification of BCES (Y|X) (Figure 1). Also, we implement comparison between methods including measurements uncertainty (York and BCES) and not including uncertainties (OLS and MA), as OLS method is still the most used linear fitting method.

Most of the tested fittings are calculated using built in packages and functions in the R programming language: OLS using lm() function, MA using lmodel2() function and York fitting using York() function from package IsoplotR. As there is no available package to calculate BCES fitting in R, BCES fitting is calculated using the lnr module in the Python programming language. Throughout the paper, uncertainties of $\delta^{13}CH_{4\ source}$ determined using different linear regressions are presented as one standard error.

OLS method minimizes the distance only on the y-axis between the fitted line and the data points, using the principle of least squares to minimize the sum of the vertical distances from the regression line, what is also known as model I regression method (Legendre and Legendre, 1998, p. chapter 10). According to Legendre and Legendre (1998), if the error rate on y-axis is more than three times than on x, OLS is the most efficient method to estimate the slope of a linear fitting.

If both x and y variables are not controlled by the researcher or measured with an error, using OLS can cause an underestimation of the slope inferred by the linear regression (Legendre and Legendre, 1998, chapter 10). Thus, the model II linear regression methods are recommended, as they minimize the distance both of x and y from the regression line. The MA method, tested in this study is an example of the model II linear regression. MA method is also known as Orthogonal Distance Regression (ODR) or Deming regression. The MA method minimizes the sum of the squared Euclidean distances (x and y distances) from the regression line. Geometric mean regression (GMR) is another model II linear regression method, but is not tested in this study as it is expected to deliver similar results to the MA method (Zobitz et al., 2006). Details about the standard errors of OLS and MA methods are presented in Appendix A.

In contrast to OLS and MA methods, York fitting (York et al., 2004) and BCES regression (Akritas and Bershady, 1993) allow inclusion of x and y uncertainties. Overall, York fitting can be treated as a general linear regression method, while OLS and MA are special cases valid in particular conditions and can be obtained mathematically from the York fitting method, when appropriate circumstances appear (York, 1966; York et al., 2004). In the York fitting method, the best slope fit is searched iteratively, where the initial slope value is assumed, e.g., using OLS. Then, computations are weighted based on x and y measurement errors. Finally, computations are repeated until differences between iteration are smaller than tolerance level (e.g., 10^{-15}) (York et al., 2004).

The BCES method is a direct extension of the OLS method and was the final linear fitting method evaluated. Within BCES, four sub-methods can be employed: BCES (Y|X), BCES (X|Y), and two symmetric lines: BCES Bisector and BCES Orthogonal (Akritas and Bershady, 1993). BCES (Y|X) assume x as the independent variable. BCES Bisector was shown to be self-inconsistent and should not be used (Hogg et al., 2010). Finally, BCES Orthogonal is a line that minimizes orthogonal distances and should be used when it is not clear which variable should be treated as the independent variable. Our study focuses on the application of BCES Orthogonal, as this method has been broadly implemented in previous studies using IRMS instruments (e.g., Fernandez et al., 2022; Lowry et al., 2020; Zazzeri et al., 2015). Additionally, to examine the difference between the two BCES methods, BCES (Y|X) is also tested, as both methods could be implemented to determine $\delta^{13}CH_4$.

To arrive at the final uncertainty of the x- and y-axis, error propagation was applied for both for Keeling and Miller-Tans methods. Details of used error propagation are presented in Appendix A.

3.5. REJECTION CRITERIA FOR AirCore SAMPLES

The determined $\delta^{13}CH_{4\ source}$ is rejected if the standard error of the fitted regression line (intercept for the Keeling method and slope for the Miller-Tans method) is greater than 5‰ (based on the Picarro CRDS performance). Based on previous studies (Defratyka 2021), an additional criterion was applied to the Miller-Tans method, where $\delta^{13}CH_{4\ source}$ is also rejected if coefficient of determination, r^2, is less than 0.85. This additional criterion was not previously applied to the Keeling method, so we examined the variance of the r^2 in the Keeling method to determine whether the r^2 criterion could also be applied.

Eventually, all retained AirCore $\delta^{13}CH_{4\ source}$ values from one data processing strategy (mass conservation approach (Sect. 3.1), background (Sect. 3.2), averaging (Sect. 3.3), and linear fitting (Sect. 3.4)) are averaged to obtain a final $\delta^{13}CH_{4\ source}$ value for each strategy. These final values are then used to compare results from different analytical approaches, presented in the flow chart on Figure 1. Additionally, for releases where bag samples for IRMS and in-situ AirCore sampling occurred simultaneously, the average AirCore results are compared with IRMS results.

4. RESULTS

Since we tested numerous techniques, as presented in flow chart in Figure 1, we present only the most meaningful results in the result section. A more exhaustive analysis can be found in Appendixes B and C. To enable comparison of results we define a reference strategy as the Miller-Tans method with individual background subtraction and the York fitting method, along with treatment 1 averaging for bag samples or raw data for AirCore.

4.1. MEASUREMENT TECHNIQUE

For bag samples measured on IRMS, a sample collected during the first day of the experiment, containing 11 µmol mol^{-1} of CH_4, biased results toward more ^{13}C enriched values and was rejected from further analysis. Potentially, observed biased came from the necessary sample dilution to obtain CH_4 mole fraction in IRMS operational range (details in Appendix B).

Due to the low mole fraction enhancement above the background, bag samples from day 2 exhibited scattered values with bias toward more ^{13}C depleted values, and were rejected from further analysis. Using remaining 18 bag samples measured on IRMS, determined $\delta^{13}CH_{4\ source}$ varied from –40.55 ± 0.12‰ (day 1) to –39.87 ± 0.10‰ (day 5), reaching treatment 1 average equal to –40.23 ± 0.14‰ and it is treated as a reference value for the other atmospheric results. In the case of samples measured with CRDS, those from day 2 were also rejected from further analysis, thus only bags collected during first day of the experiment (releases 1.1 and 1.2) were analyzed. For in-situ CRDS sampling using the AirCore tool, 3 out of 31 collected samples were rejected, due to CRDS cavity pressure and temperature instability.

Table 1 presents the comparison of determined $\delta^{13}CH_{4\ source}$ for individual releases, where sampling using two different methods was done simultaneously, and for the averaged $\delta^{13}CH_{4\ source}$ using treatment 1 averaging for all measurements techniques. Due to better instrument precision and accuracy, $\delta^{13}CH_{4\ source}$ determined using IRMS has lower uncertainty than CRDS results. From all tested measurement techniques, the uncertainty associated with bags measured by CRDS is the largest.

Averaged $\delta^{13}CH_{4\ source}$ estimates using different data processing strategies, and the result of direct $\delta^{13}CH_{4\ source}$ measurements, are presented in Figure 2, showing constant $\delta^{13}CH_{4\ source}$ from IRMS measurements using different data processing strategies. $\delta^{13}CH_{4\ source}$ measured

DATE OF SAMPLING	IRMS BAGS YORK FITTING	CRDS BAGS YORK FITTING	RESIDUAL (IRMS—CRDS BAGS)	CRDS AirCore YORK FITTING	RESIDUAL (IRMS—CRDS AirCore)
release 1.1	−40.60 ± 0.23	−41.3 ± 8.9	0.66	–	–
release 1.2	−40.56 ± 0.24	−40.8 ± 3.2	0.21	–	–
release 3.3	−40.45 ± 0.54	–	–	−40.4 ± 2.8	−0.09
all 26 releases	−40.23 ± 0.14	−41.0 ± 6.7	0.79	−41.0 ± 2.7	0.81
direct sampling	−41.36 ± 0.17				

Table 1 Comparison of direct and averaged results using bag samples measured on IRMS and CRDS (treatment 1 averaging), and CRDS AirCore samples (raw data cluster, without C_2H_6 correction). The first three rows present comparison for individual releases, where sampling using two different measurement techniques was done simultaneously. Residual between reference IRMS strategy and other analytical strategies for atmospheric measurements. 1 standard error is used as an uncertainty.

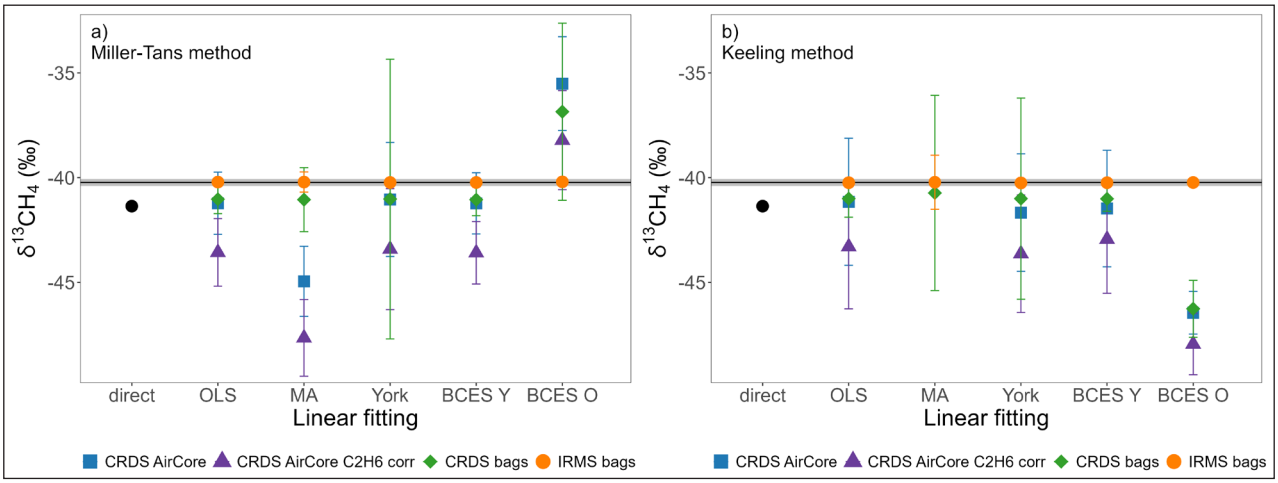

Figure 2 Comparison of direct and averaged results for different linear fitting methods. Bag samples measured on IRMS and CRDS (treatment 1 averaging), and CRDS AirCore samples (raw, non-clustered data) from mobile near-source measurements conducted during controlled release experiment. Results using Miller-Tans with individual background subtracted (left) and Keeling (right) methods are compared. Black line represents IRMS reference value with its uncertainty (gray line). For averaged $\delta^{13}CH_4$, uncertainties calculated as 1 standard error. The outlier result for MA linear fitting is not plotted. Compared linear fitting methods: OLS—Ordinary Least Squares, MA- major axis, BCES Y—Bivariate Correlated Errors and Intrinsic Scatter (Y|X) and BCES O—Bivariate Correlated Errors and Intrinsic Scatter Orthogonal.

on CRDS is more variable, depending on chosen data processing strategy (Figure 2). Using York fitting scheme as the reference linear fitting (argumentation in Sect. 4.5), for both CRDS measurement techniques, residuals from IRMS results are smaller than CRDS uncertainties. Thus, results from CRDS and IRMS instruments are in good agreement within the uncertainty. The agreement is observed for $\delta^{13}CH_{4\ source}$ determined from both individual releases and averaged $\delta^{13}CH_{4\ source}$ (Table 1).

Direct $\delta^{13}CH_{4\ source}$ measurements were more depleted (−41.36 ± 0.17‰) comparing to the atmospheric measurements. The uncertainties of direct measurements and IRMS technique are smaller than the observed discrepancy of 1.1‰ between direct and atmospheric IRMS measurements of $\delta^{13}CH_{4\ source}$. The averaged CRDS results (both for bags and AirCore samples without C_2H_6 on $\delta^{13}CH_4$ correction) are enriched about 0.3‰ comparing to direct measurements, but due to larger uncertainty of CRDS results, observed discrepancy is irrelevant within uncertainty (Figure 2).

The impact of C_2H_6 on $\delta^{13}CH_4$ correction was tested for all data processing strategies and the same trend is observed for all strategies. Thus, for simplicity the results are discussed and presented on Figure 3 only for non-clustered York fitting strategy. Applying C_2H_6 on $\delta^{13}CH_4$ corrections shifts AirCore values toward more depleted ^{13}C values, both comparing to IRMS results and to direct measurement of the cylinder batch. The residual reaches −3.2‰), and −2.05‰), comparing to bags on IRMS and direct measurements, respectively. As observed bias is significant, and deep examination of C_2H_6 on $\delta^{13}CH_4$ correction is out of scope of this study, hereafter we will mostly focus on results from AirCore samples where C_2H_6 on $\delta^{13}CH_4$ correction was not applied.

4.2. KEELING AND MILLER-TANS METHODS

Estimates of $\delta^{13}CH_{4\ source}$ determined using Miller-Tans and Keeling methods from bags measured on IRMS demonstrated insignificant difference for all applied linear fittings (Figure 2).

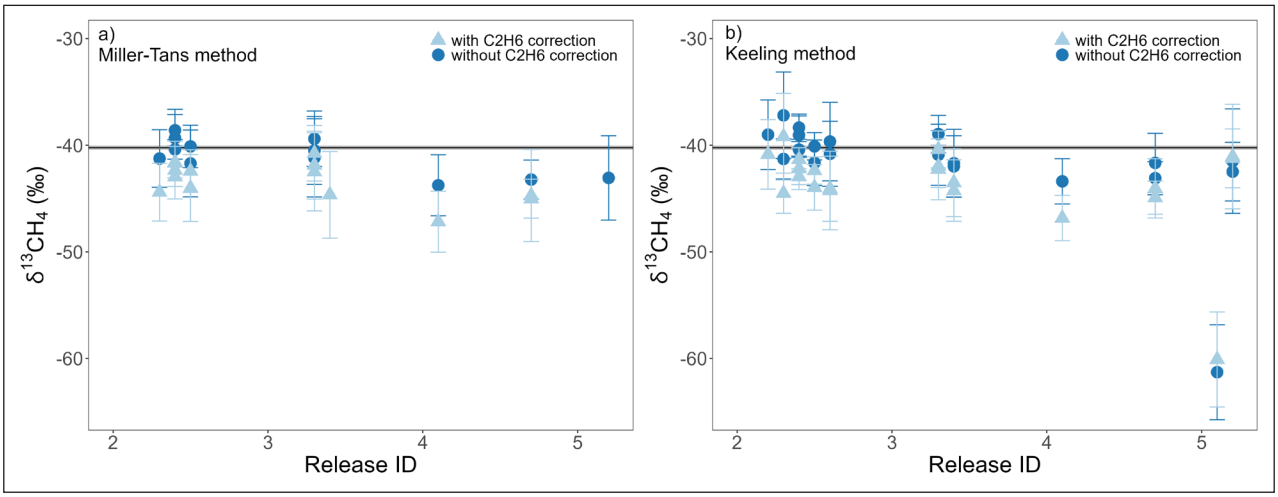

Figure 3 Individual AirCore samples with and without a C_2H_6 on $\delta^{13}CH_4$ correction from mobile near-source measurements conducted during controlled release experiment. Rejection criteria applied. For simplicity, only York fitting, and raw non-clustered data are presented, as the same trend is observed for all data processing strategies. Left: Miller-Tans with individual background subtracted method, Right: Keeling method. $\delta^{13}CH_4$ calculated as 1 standard error. Black line represents IRMS reference value with its uncertainty (gray line).

Results from bag samples measured with CRDS, using the York fitting, the $\delta^{13}CH_{4\ source}$ showed a negligible difference of 0.02‰ between $\delta^{13}CH_{4\ source}$ values determined using the Miller-Tans and Keeling method. The observed difference in determined $\delta^{13}CH_{4\ source}$ and its uncertainty varies depending on the chosen linear fitting approach. The largest discrepancy is observed when MA or BCES Orthogonal fittings are used (Figure 2).

For AirCore samples, the determined $\delta^{13}CH_{4\ source}$ showed a negligible difference of 0.2‰ for York fitting between $\delta^{13}CH_{4\ source}$ determined using the Miller-Tans and Keeling method. Similar to results from bag samples measured with CRDS, the observed difference of $\delta^{13}CH_{4\ source}$ and its uncertainty varies depending on the chosen linear fitting approach. The largest discrepancies are observed when MA (–20‰) or BCES Orthogonal (11‰) fittings are used (Figure 2). This trend is consistent regardless of whether a C_2H_6 correction on $\delta^{13}CH_4$ is applied or not (Figure 2).

4.3. BACKGROUND SUBTRACTION FOR MILLER-TANS METHOD

Using four separately defined backgrounds (individual, averaged, arbitrary I, and arbitrary II), no significant differences are observed for $\delta^{13}CH_{4\ source}$ from bag samples measured with IRMS. For $\delta^{13}CH_{4\ source}$ determined from bag samples measured with CRDS, where three different backgrounds (individual, averaged, and arbitrary I) were tested, also no impact of subtracted background was observed for all analytical strategies, except for BCES Orthogonal. A similar dependency was observed for $\delta^{13}CH_{4\ source}$ determined from AirCore samples, where individual and averaged backgrounds were subtracted. Tables of determined $\delta^{13}CH_{4\ source}$ are presented in Appendix B for bag samples and in Appendix C for AirCore samples.

4.4. DATA AVERAGING AND CLUSTERING

4.4.1. Data averaging bag samples measured by IRMS and CRDS

For analysis of bag samples measured on IRMS, the $\delta^{13}CH_{4\ source}$ reached –40.23 ± 0.14‰ using treatment 1 averaging, and –40.18 ± 0.05‰ using treatment 2 averaging. Thus, the observed discrepancy is insignificant for the IRMS study. For samples measured with CRDS, the residual difference between treatment 1 and 2 averaging was 0.3‰), and it is also insignificant.

4.4.2. Data averaging AirCore in-situ sampling

Subsequently, the impact of clustering data (using both CH_4 mole fraction and time averaging clusters) on the final, averaged $\delta^{13}CH_{4\ source}$ for AirCore samples, is presented on Figure 4. The details about clustering impact for analysis using different mass conservation methods and linear fittings can be found in Appendix C. Overall, clustering causes a changeable bias for AirCore samples, which depends on the chosen clustering strategy and the linear fitting. Additionally, clustering increases the uncertainty of the final averaged $\delta^{13}CH_{4\ source}$. Furthermore, depending on the clustering method and the linear fitting, the amount of rejected individual AirCore samples varies. For example, for York fitting, for 50 nmol mol^{-1} and 100 nmol mol^{-1} CH_4 mole fractions clusters, only one individual AirCore result remains for each cluster. The largest discrepancies between raw and clustered data are observed for the MA and BCES Orthogonal linear fitting methods, possibly due to forced symmetry applied in both methods, with $\delta^{13}CH_{4\ source}$ reaching up to –7.6 ± 2.4‰ (Figure 4).

4.5. LINEAR FITTING

Regarding the results from bag samples measured on IRMS, differences between determined $\delta^{13}CH_{4\ source}$ using

different fitting methods are insignificant (Figure 2). The largest uncertainty is observed for MA linear fitting, where uncertainty is calculated from 95% confidence intervals converted to standard error. The smallest uncertainty is observed for York fitting for both averaging approaches.

In the case of bag samples measured with CRDS, differences between determined $\delta^{13}CH_{4\ source}$ using different fitting methods are insignificant, except for results where BCES Orthogonal was used ($\delta^{13}CH_{4\ source}$ equals to −36.9 ± 3.0‰) (Figure 2). For bag samples measured on CRDS, the largest uncertainties are observed for MA and York linear fitting.

For AirCore samples, for OLS, York, and BCES (Y|X) methods, insignificant differences were observed between the Keeling and the Miller-Tans method with two distinct backgrounds, considering raw data clustering (Table 2). The results from these three linear fittings are in good agreement within each other, indicating them as good methods for AirCore data treatment. Similar to bag samples measured with CRDS, larger, and significant discrepancies were observed using MA and BCES Orthogonal methods, reaching −45.0 ± 1.7‰ and −35.5 ± 2.3‰), for raw data. Notably, only for the BCES Orthogonal fitting, the results from Miller-Tans methods with two differently defined backgrounds were significantly different.

4.6. REJECTION CRITERIA

Previous research using the Miller-Tans method proposed to reject individual AirCore sample results if their uncertainty is greater than 5‰), and if r^2 is less than 0.85 (Defratyka et al., 2021). The fraction of rejected AirCore predictably varied with the data processing strategy (Table 2 and more details in Appendix C). For example, using the reference analytical strategy, 12 out of the 28 AirCore samples remained, after applying the rejection criteria.

We investigated whether the same rejection criteria can be applied to the Keeling method. For the CRDS AirCore studies, the r^2 values remain scattered, regardless of whether determined $\delta^{13}CH_{4\ source}$ agreed with IRMS reference value or not. Also, r^2 remains systematically low, mostly ranging between 0.1 and 0.3. Thus, it was not possible to find a satisfying r^2 rejection criterion for

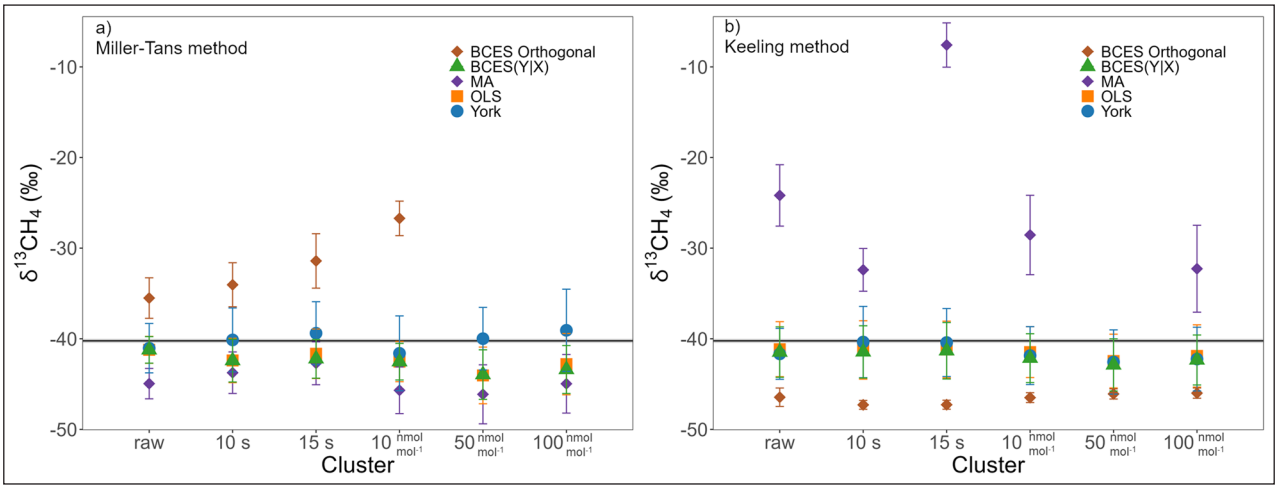

Figure 4 Comparison of averaged CRDS AirCore samples for different cluster averaging from mobile near-source measurements conducted during controlled release experiment. C_2H_6 correction was not applied. Results using Miller-Tans with individual background subtracted (left) and Keeling (right) methods are compared. $\delta^{13}CH_4$, uncertainties calculated as 1 standard error. Black line represents IRMS reference value with its uncertainty (gray line). Compared linear fitting methods: OLS—Ordinary Least Squares, MA- major axis, BCES Y—Bivariate Correlated Errors and Intrinsic Scatter (Y|X) and BCES O—Bivariate Correlated Errors and Intrinsic Scatter Orthogonal.

LINEAR FITTING	$\delta^{13}CH_4$ ± U($\delta^{13}CH_4$) (‰)			$n_{AirCore}$ KEELING METHOD	$n_{AirCore}$ MILLER-TANS 1	$n_{AirCore}$ MILLER-TANS 2
	KEELING METHOD	MILLER-TANS METHOD 1	MILLER-TANS METHOD 2			
OLS	−41.1 ± 3.0	−41.2 ± 1.5	−41.2 ± 1.5	22	12	12
MA	−24.2 ± 3.4	−45.0 ± 1.7	−45.0 ± 1.7	2	12	12
York	−41.7 ± 2.8	−41.0 ± 2.7	−40.9 ± 2.1	21	12	12
BCES Orthogonal	−46.5 ± 1.0	−35.5 ± 2.2	−39.8 ± 1.9	19	9	12
BCES (Y|X)	−41.4 ± 2.8	−41.2 ± 1.5	−41.2 ± 1.5	25	12	12

Table 2 CRDS AirCore samples for raw cluster data. $n_{AirCore}$ represents number of AirCore samples used to determine averaged $\delta^{13}CH_4$ after applying rejection criteria. C_2H_6 on $\delta^{13}CH_4$ correction not applied; one standard error is used as an uncertainty.

Keeling method. Applying only the uncertainty criterion leads to fewer rejections and a wider spread of $\delta^{13}CH_{4\ source}$ among individual AirCore samples using the Keeling method, which therefore increases the uncertainty of the final, averaged $\delta^{13}CH_{4\ source}$ (Figure 4).

5. DISCUSSION

5.1. COMPARISON WITH PREVIOUS STUDIES

A few studies have been conducted to find the best strategy for applying the Keeling or the Miller-Tans methods to determine isotopic signatures, and they focused mostly on synthetic data or continuous measurements of CO_2 (Miller and Tans, 2003; Pataki et al., 2003; Wehr and Saleska, 2017; Zobitz et al., 2006). Furthermore, Hoheisel et al. (2019), focused on atmospheric CH_4 measurements, using both CRDS AirCore sampling and synthetic data to compare use of OLS and York fitting during the application of the Keeling and Miller-Tans method. Pataki et al. (2003) concentrated on the application of the Keeling method for $\delta^{13}C$ of CO_2. However, as they highlighted in their paper, this method can be used also for other gas species or isotopes, where each application has its own constraints. Pataki et al. (2003) and Miller and Tans (2003) recommend using the model II (e.g. MA) fitting method for mass conservation because the OLS method could introduce a systematic bias, especially if the linear fitting r^2 value is low. However, Zobitz et al. (2006) showed that model II can also introduce some bias if the range of the CO_2 mole fraction is low (e.g., CO_2 enhancement above background is lower than 20 µmol mol^{-1}) and if variability on the x-axis is much lower than in the y-axis. Geometric mean regression (GMR) is another model II linear regression method that was not tested in our study, as it is expected to yield similar results to the MA method (Zobitz et al., 2006). In our study, we observed bias in the MA method for CRDS studies, where the uncertainty and fluctuation of the measured $\delta^{13}CH_{4\ obs}$ were greater than those for $CH_{4\ obs}$ mole fractions. As advised by Hoheisel et al. (2019), we focused on releases where the measured CH_4 mole fraction exceeded the background mole fraction by at least 0.5 µmol mol^{-1}. This provided a signal-to-noise ratio large enough to avoid introducing biases in high precision IRMS measurements using the model II method. However, bias due to low signal-to-noise ratio can occur when observing lower enhancements. This is typically the case for measurement stations conducting continuous measurements located at some distance from the source.

Hoheisel et al. (2019) focused on the comparison of the Keeling and Miller-Tans methods, using OLS and York fittings, for $CH_{4\ obs}$ AirCore and synthetic data. Regarding the comparison of measurement techniques, they obtained identical results for the Keeling and Miller-Tans methods when using York fitting. Using OLS fitting, they observed differences from –2‰ to 2‰ for individual AirCore samples between the Keeling and Miller-Tans methods. Hoheisel et al. (2019) showed that for AirCore studies, the results from York fitting fall between results obtained using OLS with the Keeling or Miller-Tans method for 90% of the measurements. In their study, results from York and OLS are nearly the same, but both show larger differences from the true, modeled value than from each other. The observed discrepancy between the fitted and true value reached <0.2‰ These results are consistent with our study, where we did not observe significant differences between York and OLS fittings and similar discrepancies between AirCore samples and direct $\delta^{13}CH_{4\ source}$. Moreover, Hoheisel et al. (2019) investigated the influence of averaging time, examining intervals up to 1 minute. Using synthetic data, they demonstrated no significant differences between raw and 15 s averaged. They also observed improved precision of the measurements when averaging over 1 minute, but this did not enhance the determination of $\delta^{13}CH_{4\ source}$. This contrasts with our results from mobile measurements, where we observed a varying bias introduced by data averaging, using different clusters, which worsens the determination of the final $\delta^{13}CH_{4\ source}$ (Figure 4).

We found that implementing a C_2H_6 correction on $\delta^{13}CH_4$ (as described in other studies) introduces a possible bias, resulting in the final averaged $\delta^{13}CH_4$ to be more ^{13}C depleted than calculated from IRMS measurements or from measurements made directly from the cylinder batch. To our knowledge, this is the first study to directly compare CRDS AirCore results with $\delta^{13}CH_{4\ source}$ determined from bag samples measured on an IRMS and direct source sampling, providing evidence to exclude a C_2H_6 correction for measuring $\delta^{13}CH_4$ in these types of samples. Previous studies that implemented a C_2H_6 correction focused solely on CRDS AirCore measurements, without the comparing them to independent C_2H_6-interference free measurements (Assan et al., 2017; Hoheisel et al., 2019; Lopez et al., 2017; Rella et al., 2015).

Finally, several studies, including Wehr and Saleska (2017) and Hoheisel et al. (2019), proposed using York fitting to determine $\delta^{13}CH_{4\ source}$, as it is the most general regression method, which also accounts for uncertainties of both the x- and the y-axis. Based on Monte Carlo simulations, used to determine the isotopic signatures of CO_2, Wehr and Saleska (2017) presented that York fitting produces the closest realistic results, compared to OLS and GMR methods. Their conclusion aligns with our study, as the York fitting method consistently provides robust results for all examined analytical approaches. Additionally, we observe smaller discrepancies between the OLS and York fitting methods compared to the studies of Wehr and Saleska (2017). This can be explained by the larger CH_4 enhancements relative to CO_2 enhancements

experienced in our study compared to theirs. Notably, we also tested the BCES linear fitting using two sub-methods: BCES (Y|X) and BCES Orthogonal, which had not been previously tested for atmospheric applications. We demonstrated that the choice of linear fitting method does not affect IRMS results. For AirCore samples, BCES (Y|X) results are in good agreement with York fitting results, whereas BCES Orthogonal introduces significant bias and should not be used for AirCore samples.

5.2. POSSIBLE IMPROVEMENTS AND FURTHER APPLICATIONS

Based on our study, several analytical details warrant special attention during the determination of $\delta^{13}CH_{4\ source}$. We observed that individual AirCore values for samples collected on days 4 and 5 of the controlled release experiment were more depleted compared to samples collected from days 2 and 3 (Figure 3) and from the reference IRMS value. It is possible that an unnoticed issue, such as a leak, may have occurred during those days. Therefore, we recommend measuring calibration and working target gases on each measurement day, both before and after the fieldwork.

We observed about a 1.1‰ discrepancy in IRMS results between atmospheric and directly determined $\delta^{13}CH_{4\ source}$. This discrepancy could be caused by different conditions in which direct and atmospheric samples were collected. For atmospheric studies, the gas was released over 45 minutes from the cylinder at high rates (up to 70 l min^{-1}) and was sampled in a downwind plume up to 250 m from the release position. For direct sampling, gas was transferred from cylinder batch to 10 L cylinder in less than two minutes. During the controlled release experiment, we did not observe significant differences or trends between atmospheric $\delta^{13}CH_{4\ source}$ determined during different releases, even when CH_4 flow rate, wind speed, or wind direction varied. These physical phenomena alone only impact the dispersion characteristic of CH_4 from the source to the sampling location, without any plausible mechanism for isotopic fractionation within the boundary layer on these short timescales. Further studies on possible isotopic fractionation during gas release are planned in the future to verify observed discrepancy.

In our study, we focus entirely on finding the best data processing strategy for near-source mobile measurements to determine $\delta^{13}CH_{4\ source}$. However, we anticipate that the results can be generalized to other applications where similar isotopic mixing lines are appropriate. For example, the same conclusions should apply for the determination of δD-CH_4 and stable isotope ratios of CO_2. Also, our conclusions should be applicable for continuous isotopic measurements, both for CO_2 and CH_4. Before expanding our conclusion to other isotopes or continuous measurement studies, it is important to consider that the range of observed mole fractions, signal-to-noise ratios, precision, and variability of the y-axis could potentially introduce biases depending on their magnitudes and on the chosen fitting methods. Based on our study, York, and BCES (Y|X) are good candidate methods to apply in different contexts, as they exhibited the least variability and incorporate uncertainties of the x- and y-axis. Furthermore, establishing rejection criteria for individual applications, such as the size of uncertainty or the r^2 parameter, can identify outliers and improve the accuracy and precision of determining $\delta^{13}CH_{4\ source}$ isotopic signatures.

6. CONCLUSIONS AND RECOMMENDATIONS

Our study aims to find the most robust data processing strategy for determining $\delta^{13}CH_{4\ source}$ isotopic signatures from mobile measurements, while eliminating the need to choose between biased methods or switch between methods depending on the conditions. With the increasing popularity of CRDS instruments for measuring source signatures, it is crucial to evaluate comparatively the performance of both IRMS and CRDS for determining $\delta^{13}CH_{4\ source}$. The novelty of the study is the comprehensive inter-comparison between atmospheric studies of $\delta^{13}CH_4$ using (i) bag sampling measured afterwards both by IRMS and CRDS, (ii) in-situ CRDS with an AirCore storage tool under controlled release conditions. Also, we focused on intercomparison of different analytical strategies used in atmospheric studies of $\delta^{13}CH_{4\ source}$. We tested aspects not detailed in previous studies, such as background subtraction, data averaging, and BCES linear fitting. To achieve this, we focused on data from a controlled release experiment, which simulates real-life methane point sources, such as leaks in natural gas infrastructure. This approach enables the validation and implementation of conclusions from studies primarily focused on synthetic or CO_2 data (Miller and Tans, 2003; Pataki et al., 2003; Wehr and Saleska, 2017; Zobitz et al., 2006).

The chosen mass balance approach and linear fitting method do not significantly affect IRMS results (Figure 2). The high precision and accuracy of IRMS instruments lead to a more reproducible estimation of the $\delta^{13}CH_4$ signature than from CRDS measurements. There is no significant difference observed with background subtraction for the Miller-Tans method; however, for the consistency, individual backgrounds should be subtracted. Bag samples collected on different days should not be treated as one dataset. Instead, $\delta^{13}CH_{4\ source}$ should be calculated for individual days and then averaged.

In contrast, $\delta^{13}CH_{4\ source}$ measurements are more sensitive to data processing choices for CRDS than for IRMS measurement technique. Estimates of $\delta^{13}CH_{4\ source}$ determined using in-situ CRDS AirCore measurements agrees well with the IRMS results, when York fitting method is used. The addition of an AirCore unambiguously

provides more robust results and should be implemented for in-situ CRDS measurements.

For CRDS AirCore studies, we recommend using the Miller-Tans method, with the subtraction of the individual backgrounds. To achieve robust and accurate results, raw, non-clustered data should be analyzed. For consistency, we recommend using either York or BCES (Y|X) fitting methods for both IRMS bag samples and CRDS AirCore, as they include the uncertainty of measurement points and give the most consistent results. The OLS method can also be applied to determine $\delta^{13}CH_{4\ source}$, as differences between York, BCES (Y|X), and OLS fitting methods are not significant within the uncertainty range. However, in the cases of lower CH_4 range or higher uncertainty in the measured $\delta^{13}CH_{4\ source,}$ the discrepancy between York and OLS methods may increase. For CRDS AirCore studies, we strongly discourage the use of the MA and BCES Orthogonal methods, as their forced symmetry introduces varying biases (Figure 4). Adhering to these recommendations will reduce the risk of obtaining inaccurate and imprecise $\delta^{13}CH_{4\ source}$ isotopic signatures.

The conclusions of our work provide a robust starting point for other applications that utilize isotopic mixing lines. However, the range of observed mole fractions, signal-to-noise ratios, and precision and fluctuation of isotopic signatures have the potential to introduce biases depending on their magnitude and the chosen data processing strategy. Thus, as demonstrated in this study, the applied data processing strategy must be chosen carefully.

DATA ACCESSIBILITY STATEMENT

The data that support the findings of this study are openly available in Defratyka, Sara (2023), 'Dataset: Statistical evaluation of methane isotopic signatures determined during near-source measurements,' Mendeley Data, V1, doi: 10.17632/vfbbdvp9w2.1 at https://data.mendeley.com/datasets/vfbbdvp9w2/1.

ADDITIONAL FILE

The additional file for this article can be found as follows:

- **Supplement Information.** Appendix A to C and Supplementary References. DOI: https://doi.org/10.16993/tellusb.1878.s1

FUNDING INFORMATION

This research has been supported by the European Union's Horizon 2020 research and innovation program (Marie Skłodowska-Curie grant no. 722479).

The controlled release experiment was part of the NERC grant New methodologies for removal of methane from the atmosphere (NE/P019641/1), which also funded the LGR UMEA instrument used in these experiments. RHUL participation in the experiment was funded by the NERC Equipt4Risk project (NE/R017360/1).

TA and CR acknowledge funding from 21GRD04 isoMET. 21GRD04 isoMET has received funding from the European Partnership on Metrology, co-financed from the European Union's Horizon Europe Research and Innovation Programme and by the Participating States.

COMPETING INTERESTS

The authors have no competing interests to declare.

AUTHOR CONTRIBUTIONS

S.M.D: Writing—original draft, Conceptualization, Visualization, Methodology, Validation, Formal analysis, Data curation, Investigation. **J.L.F:** Conceptualization, Methodology, Investigation, Data Curation, Writing—review and editing. **R.E.F:** Conceptualization, Methodology, Validation, Resources, Writing—review and editing. **D.L.:** Conceptualization, Methodology, Validation, Resources, Writing—review and editing. **J.M.F:** Investigation, Data Curation, Formal analysis, Writing—review and editing. **S.B:** Investigation, Data Curation, Writing—review and editing. **C.Y.K:** Supervision, Methodology, Validation, Resources, Writing—review and editing. **J.D.P:** Supervision, Validation. **P.B:** Supervision, Conceptualization, Methodology, Validation, Resources, Writing—review and editing. **T.A:** Supervision, Methodology, Validation, Writing—review and editing. **C.R:** Methodology, Validation, **J.H:** Conceptualization, Methodology, Validation, Investigation, Writing—review and editing. **N.Y:** Conceptualization, Methodology, Validation, Investigation. **E.G.N:** Writing—review and editing.

AUTHOR AFFILIATIONS

Sara M. Defratyka orcid.org/0000-0002-9488-4518
School of GeoSciences, University of Edinburgh, Edinburgh, UK; National Physical Laboratory, Hampton Road, Teddington, UK

James L. France orcid.org/0000-0002-8785-1240
Department of Earth Sciences, Royal Holloway, University of London, UK; Environmental Defense Fund, UK

Rebecca E. Fisher orcid.org/0000-0002-9262-5467
Department of Earth Sciences, Royal Holloway, University of London, UK

Dave Lowry orcid.org/0000-0002-8535-0346
Department of Earth Sciences, Royal Holloway, University of London, UK

Julianne M. Fernandez orcid.org/0000-0001-5137-6620
Scientific Aviation, Inc., USA

Semra Bakkaloglu orcid.org/0000-0002-0476-1929
Department of Chemical Engineering, Imperial College London, London SW7 2 AZ, UK

Camille Yver-Kwok orcid.org/0000-0002-2181-2863
Laboratoire des Sciences du Climat et de l'Environnement (LSCE-IPSL) CEA-CNRS-UVSQ, Université Paris Saclay, France

Jean-Daniel Paris orcid.org/0000-0003-2164-4916
Laboratoire des Sciences du Climat et de l'Environnement (LSCE-IPSL) CEA-CNRS-UVSQ, Université Paris Saclay, France

Philippe Bousquet orcid.org/0000-0002-4444-2703
Laboratoire des Sciences du Climat et de l'Environnement (LSCE-IPSL) CEA-CNRS-UVSQ, Université Paris Saclay, France

Tim Arnold orcid.org/0000-0001-9097-8907
School of GeoSciences, University of Edinburgh, Edinburgh, UK; Department of Physical Geography and Ecosystem Science, Lund University, Sweden

Chris Rennick orcid.org/0000-0003-4993-0156
National Physical Laboratory, Hampton Road, Teddington, UK

Jon Helmore orcid.org/0009-0005-1325-6982
National Physical Laboratory, Hampton Road, Teddington, UK

Nigel Yarrow orcid.org/0009-0009-1568-9342
National Physical Laboratory, Hampton Road, Teddington, UK

Euan G. Nisbet orcid.org/0000-0001-8379-857X
Department of Earth Sciences, Royal Holloway, University of London, UK

REFERENCES

Akritas, M.G. and **Bershady, M.A.** (1993) Linear regression for astronomical data with measurement errors and intrinsic scatter. *Astrophys. J.*, 420(2): 706–714. DOI: https://doi.org/10.1086/177901

Al-Shalan, A., Lowry, D., Fisher, R.E., Nisbet, E.G., Zazzeri, G., Al-Sarawi, M. and **France, J.L.** (2022) Methane emissions in Kuwait: Plume identification, isotopic characterisation and inventory verification. *Atmos. Environ.*, 268: 118763. DOI: https://doi.org/10.1016/j.atmosenv.2021.118763

Assan, S., Baudic, A., Guemri, A., Ciais, P., Gros, V. and **Vogel, F.R.** (2017) Characterization of interferences to in situ observations of d13CH4 and C2H6 when using a cavity ring-down spectrometer at industrial sites. *Atmospheric Meas. Tech.*, 10: 2077–2091. DOI: https://doi.org/10.5194/amt-10-2077-2017

Bakkaloglu, S., Lowry, D., Fisher, R.E., France, J.L. and **Nisbet, E.G.** (2021) Carbon isotopic characterisation and oxidation of UK landfill methane emissions by atmospheric measurements. *Waste Manag.*, 132: 162–175. DOI: https://doi.org/10.1016/j.wasman.2021.07.012

Bakkaloglu, S., Lowry, D., Fisher, R.E., Menoud, M., Lanoisellé, M., Chen, H., Röckmann, T. and **Nisbet, E.G.** (2022) Stable isotopic signatures of methane from waste sources through atmospheric measurements. *Atmos. Environ.*, 276: 119021. DOI: https://doi.org/10.1016/j.atmosenv.2022.119021

Basu, S., Lan, X., Dlugokencky, E., Michel, S., Schwietzke, S., Miller, J.B., Bruhwiler, L., Oh, Y., Tans, P.P., Apadula, F., Gatti, L.V., Jordan, A., Necki, J., Sasakawa, M., Morimoto, S., Di Iorio, T., Lee, H., Arduini, J. and **Manca, G.** (2022) Estimating emissions of methane consistent with atmospheric measurements of methane and δ13C of methane. *Atmospheric Chem. Phys.*, 22: 15351–15377. DOI: https://doi.org/10.5194/acp-22-15351-2022

Brownlow, R., Lowry, D., Fisher, R.E., France, J.L., Lanoisellé, M., White, B., Wooster, M.J., Zhang, T. and **Nisbet, E.G.** (2017) Isotopic ratios of tropical methane emissions by atmospheric measurement: Tropical methane δ13C source signatures. *Glob. Biogeochem. Cycles*, 31: 1408–1419. DOI: https://doi.org/10.1002/2017GB005689

Chanton, J.P., Rutkowski, C.M., Schwartz, C.C., Ward, D.E. and **Boring, L.** (2000) Factors influencing the stable carbon isotopic signature of methane from combustion and biomass burning. *J. Geophys. Res. Atmospheres*, 105: 1867–1877. DOI: https://doi.org/10.1029/1999JD900909

Craig, H. (1957) Isotopic standards for carbon and oxygen and correctiofna ctors for mass-spectrometric analysis of carbon dioxide. *Geochim. Cosmochim. Acta.*, 12: 133–149. DOI: https://doi.org/10.1016/0016-7037(57)90024-8

Defratyka, S. (2021) Characterizing methane (CH4) emissions in urban environments (Paris). Ph.D. Thesis. Université Paris-Saclay. NNT: 2021UPASJ002. Available at https://theses.hal.science/tel-03230140/ (Accessed: 03.02.2025)

Defratyka, S. (2023) Dataset: Statistical evaluation of methane isotopic signatures determined during near-source measurements. *Mendeley Data*, V1. DOI: https://doi.org/10.17632/vfbbdvp9w2.1

Defratyka, S.M., Paris, J.-D., Yver-Kwok, C., Fernandez, J.M., Korben, P. and **Bousquet, P.** (2021) Mapping urban methane sources in Paris, France. *Environ. Sci. Technol.*, 55: 8583–8591. DOI: https://doi.org/10.1021/acs.est.1c00859

Dlugokencky, E.J. (2022) *NOAA/ESRL*. Available at https://gml.noaa.gov/ccgg/trends_ch4/ [Last accessed 03 February 2025].

Fernandez, J.M., Maazallahi, H., France, J.L., Menoud, M., Corbu, M., Ardelean, M., Calcan, A., Townsend-Small, A., van der Veen, C., Fisher, R.E., Lowry, D., Nisbet, E.G. and **Röckmann, T.** (2022) Street-level methane emissions of Bucharest, Romania and the dominance of urban wastewater. *Atmospheric Environ. X*, 13: 100153. DOI: https://doi.org/10.1016/j.aeaoa.2022.100153

Fisher, R., Lowry, D., Wilkin, O., Sriskantharajah, S. and **Nisbet, E.G.** (2006) High-precision, automated stable isotope analysis of atmospheric methane and carbon dioxide using continuous-flow isotope-ratio mass spectrometry. *Rapid Commun. Mass Spectrom.*, 20: 200–208. DOI: https://doi.org/10.1002/rcm.2300

France, J.L., Cain, M., Fisher, R.E., Lowry, D., Allen, G., O'Shea, S.J., Illingworth, S., Pyle, J., Warwick, N., Jones, B.T., Gallagher, M.W., Bower, K., Le Breton, M., Percival, C., Muller, J., Welpott, A., Bauguitte, S., George, C., Hayman, G.D., Manning, A.J., Myhre, C.L., Lanoisellé, M. and **Nisbet, E.G.** (2016) Measurements of δ13C in CH4 and using particle dispersion modeling to characterize sources of Arctic methane within an air mass. *J. Geophys. Res. Atmospheres*, 121,14, 257–14,270. DOI: https://doi.org/10.1002/2016JD026006

Gardiner, T., Helmore, J., Innocenti, F. and **Robinson, R.** (2017) Field validation of remote sensing methane emission measurements. *Remote Sens.*, 9: 956. DOI: https://doi.org/10.3390/rs9090956

Germain-Piaulenne, E., Paris, J.-D., Gros, V., Quehe, P.-Y., Pikridas, M., Baisnee, D., Berchet, A., Sciare, J. and **Bourtsoukidis, E.** (2024) Middle East oil and gas methane emissions signature captured at a remote site using light hydrocarbon tracers. *Atmos. Environ.* 22: 100253. DOI: https://doi.org/10.1016/j.aeaoa.2024.100253

Hogg, D.W., Bovy, J. and **Lang, D.** (2010) Data analysis recipes: Fitting a model to data. ArXiv10084686 Astro-Ph Physicsphysics. [Last accessed 03 February 2025].

Hoheisel, A., Yeman, C., Dinger, F., Eckhardt, H. and **Schmidt, M.** (2019) An improved method for mobile characterisation of D13CH4 source signatures and its application in Germany. *Atmospheric Meas. Tech.*, 12: 1123–1139. DOI: https://doi.org/10.5194/amt-12-1123-2019

Karion, A., Sweeney, C., Tans, P. and **Newberger, T.** (2010) AirCore: An innovative atmospheric sampling system. *J. Atmospheric Ocean. Technol.*, 27(11): 1839–1853. DOI: https://doi.org/10.1175/2010JTECHA1448.1

Keeling, C.D. (1961) The concentration and isotopic abundances of carbon dioxide in rural and marine air. *Geochim. Cosmochim. Acta*, 24: 277–298. DOI: https://doi.org/10.1016/0016-7037(61)90023-0

Lan, X., Basu, S., Schwietzke, S., Bruhwiler, L.M.P., Dlugokencky, E.J., Michel, S.E., Sherwood, O.A., Tans, P.P., Thoning, K., Etiope, G., Zhuang, Q., Liu, L., Oh, Y., Miller, J.B., Pétron, G., Vaughn, B.H. and **Crippa, M.** (2021) Improved constraints on global methane emissions and sinks using δ13C-CH4. *Glob. Biogeochem. Cycles*, 35: e2021GB007000. DOI: https://doi.org/10.1029/2021GB007000

Legendre, P. and **Legendre, L.** (1998) *Numerical ecology, second English ed*. Amsterdam: Elsevier Science B.V.

Lopez, M., Sherwood, O.A., Dlugokencky, E.J., Kessler, R., Giroux, L. and **Worthy, D.E.J.** (2017) Isotopic signatures of anthropogenic CH4 sources in Alberta, Canada. *Atmos. Environ.*, 164: 280–288. DOI: https://doi.org/10.1016/j.atmosenv.2017.06.021

Lowry, D., Fisher, R.E., France, J.L., Coleman, M., Lanoisellé, M., Zazzeri, G., Nisbet, E.G., Shaw, J.T., Allen, G., Pitt, J. and **Ward, R.S.** (2020) Environmental baseline monitoring for shale gas development in the UK: Identification and geochemical characterisation of local source emissions of methane to atmosphere. *Sci. Total Environ.*, 708: 134600. DOI: https://doi.org/10.1016/j.scitotenv.2019.134600

Maazallahi, H., Fernandez, J.M., Menoud, M., Zavala-Araiza, D., Weller, Z.D., Schwietzke, S., von Fischer, J.C., Denier van der Gon, H. and **Röckmann, T.** (2020) Methane mapping, emission quantification, and attribution in two European cities: Utrecht (NL) and Hamburg (DE). *Atmospheric Chem. Phys.*, 20: 14717–14740. DOI: https://doi.org/10.5194/acp-20-14717-2020

Menoud, M., Morales, R.P., Pison, I., Bousquet, P. and **Röckmann, T.** (2020) Characterisation of methane sources in Lutjewad, The Netherlands, using quasi-continuous isotopic composition measurements. *Tellus B*, 72: 1, 1–20. DOI: https://doi.org/10.1080/16000889.2020.1823733

Menoud, M., van der Veen, C., Lowry, D., Fernandez, J.M., Bakkaloglu, S., France, J.L., Fisher, R.E., Maazallahi, H., Stanisavljević, M., Nęcki, J., Vinkovic, K., Łakomiec, P., Rinne, J., Korbeń, P., Schmidt, M., Defratyka, S., Yver-Kwok, C., Andersen, T., Chen, H. and **Röckmann, T.** (2022) New contributions of measurements in Europe to the global inventory of the stable isotopic composition of methane. *Earth Syst. Sci. Data*, 14: 4365–4386. DOI: https://doi.org/10.5194/essd-14-4365-2022

Menoud, M., van der Veen, C., Necki, J., Bartyzel, J., Szénási, B., Stanisavljević, M., Pison, I., Bousquet, P. and **Röckmann, T.** (2021) Methane (CH4) sources in Krakow, Poland: insights from isotope analysis. *Atmospheric Chem. Phys.*, 21: 13167–13185. DOI: https://doi.org/10.5194/acp-21-13167-2021

Miller, J.B. and **Tans, P.P.** (2003) Calculating isotopic fractionation from atmospheric measurements at various scales. *Tellus B Chem. Phys. Meteorol.*, 55(2): 207–214. DOI: https://doi.org/10.3402/tellusb.v55i2.16697

Pataki, D.E., Ehleringer, J.R., Flanagan, L.B., Yakir, D., Bowling, D.R., Still, C.J., Buchmann, N., Kaplan, J.O. and **Berry, J.A.** (2003) The application and interpretation of Keeling plots in terrestrial carbon cycle research: APPLICATION OF KEELING PLOTS. *Glob. Biogeochem. Cycles*, 17(1): 1022. DOI: https://doi.org/10.1029/2001GB001850

Phillips, N.G., Ackley, R., Crosson, E.R., Down, A., Hutyra, L.R., Brondfield, M., Karr, J.D., Zhao, K. and **Jackson, R.B.** (2013) Mapping urban pipeline leaks: Methane leaks across *Boston. Environ. Pollut.*, 173: 1–4. DOI: https://doi.org/10.1016/j.envpol.2012.11.003

Rella, C.W., Hoffnagle, J., He, Y. and **Tajima, S.** (2015) Local- and regional-scale measurements of CH4, d13CH4, and C2H6; in the Uintah Basin using a mobile stable isotope analyzer. *Atmospheric Meas. Tech.*, 8: 4539–4559. DOI: https://doi.org/10.5194/amt-8-4539-2015

Rennick, C., Arnold, T., Safi, E., Drinkwater, A., Dylag, C., Webber, E.M., Hill-Pearce, R., Worton, D.R., Bausi, F. and **Lowry, D.** (2021) Boreas: A sample preparation-coupled laser spectrometer system for simultaneous high-precision in situ analysis of δ13C and δ2H from ambient air methane. *Anal. Chem.*, 93: 10141–10151. DOI: https://doi.org/10.1021/acs.analchem.1c01103

Rigby, M., Manning, A.J. and **Prinn, R.G.** (2012) The value of high-frequency, high-precision methane isotopologue measurements for source and sink estimation: METHANE ISOTOPOLOGUES IN INVERSIONS. *J. Geophys. Res. Atmospheres*, 117: D12312. DOI: https://doi.org/10.1029/2011JD017384

Röckmann, T., Eyer, S., van der Veen, C., Popa, M.E., Tuzson, B., Monteil, G., Houweling, S., Harris, E., Brunner, D., Fischer, H., Zazzeri, G., Lowry, D., Nisbet, E.G., Brand, W.A., Necki, J.M., Emmenegger, L. and **Mohn, J.** (2016) In situ observations of the isotopic composition of methane at the Cabauwtall tower site. *Atmospheric Chem. Phys.*, 16: 10469–10487. DOI: https://doi.org/10.5194/acp-16-10469-2016

Saunois, M., Stavert, A.R., Poulter, B., Bousquet, P., Canadell, J.G., Jackson, R.B., Raymond, P.A., Dlugokencky, E.J., Houweling, S., Patra, P.K., Ciais, P., Arora, V.K., Bastviken, D., Bergamaschi, P., Blake, D.R., Brailsford, G., Bruhwiler, L., Carlson, K.M., Carrol, M., Castaldi, S., Chandra, N., Crevoisier, C., Crill, P.M., Covey, K., Curry, C.L., Etiope, G., Frankenberg, C., Gedney, N., Hegglin, M.I., Höglund-Isaksson, L., Hugelius, G., Ishizawa, M., Ito, A., Janssens-Maenhout, G., Jensen, K.M., Joos, F., Kleinen, T., Krummel, P.B., Langenfelds, R.L., Laruelle, G.G., Liu, L., Machida, T., Maksyutov, S., McDonald, K.C., McNorton, J., Miller, P.A., Melton, J.R., Morino, I., Müller, J., Murguia-Flores, F., Naik, V., Niwa, Y., Noce, S., O'Doherty, S., Parker, R.J., Peng, C., Peng, S., Peters, G.P., Prigent, C., Prinn, R., Ramonet, M., Regnier, P., Riley, W.J., Rosentreter, J.A., Segers, A., Simpson, I.J., Shi, H., Smith, S.J., Steele, L.P., Thornton, B.F., Tian, H., Tohjima, Y., Tubiello, F.N., Tsuruta, A., Viovy, N., Voulgarakis, A., Weber, T.S., van Weele, M., van der Werf, G.R., Weiss, R.F., Worthy, D., Wunch, D., Yin, Y., Yoshida, Y., Zhang, W., Zhang, Z., Zhao, Y., Zheng, B., Zhu, Qing, Zhu, Qiuan and **Zhuang, Q.** (2020) The global methane budget 2000–2017. *Earth Syst. Sci. Data*, 12: 1561–1623. DOI: https://doi.org/10.5194/essd-12-1561-2020

Schwietzke, S., Sherwood, O.A., Bruhwiler, L.M.P., Miller, J.B., Etiope, G., Dlugokencky, E.J., Michel, S.E., Arling, V.A., Vaughn, B.H., White, J.W.C. and **Tans, P.P.** (2016) Upward revision of global fossil fuel methane emissions based on isotope database. *Nature*, 538: 88–91. DOI: https://doi.org/10.1038/nature19797

Sherwood, O.A., Schwietzke, S., Arling, V.A. and **Etiope, G.** (2017) Global inventory of gas geochemistry data from fossil fuel, microbial and burning sources, version 2017. *Earth Syst. Sci. Data*, 9: 639–656. DOI: https://doi.org/10.5194/essd-9-639-2017

Simpson, I.J., Sulbaek Andersen, M.P., Meinardi, S., Bruhwiler, L., Blake, N.J., Helmig, D., Rowland, F.S. and **Blake, D.R.** (2012) Long-term decline of global atmospheric ethane concentrations and implications for methane. *Nature*, 488: 490–494. DOI: https://doi.org/10.1038/nature11342

Townsend-Small, A., Ferrara, T.W., Lyon, D.R., Fries, A.E. and **Lamb, B.K.** (2016) Emissions of coalbed and natural gas methane from abandoned oil and gas wells in the United States. *Geophys. Res. Lett.*, 43: 2283–2290. DOI: https://doi.org/10.1002/2015GL067623

Townsend-Small, A., Tyler, S.C., Pataki, D.E., Xu, X. and **Christensen, L.E.** (2012) Isotopic measurements of atmospheric methane in Los Angeles, California, USA: Influence of "fugitive" fossil fuel emissions: Los Angeles methane emissions. *J. Geophys. Res. Atmospheres*, 117: D07308. DOI: https://doi.org/10.1029/2011JD016826

Turner, A.J., Frankenberg, C. and **Kort, E.A.** (2019). Interpreting contemporary trends in atmospheric methane. *Proc. Natl. Acad. Sci.*, 116: 2805–2813. DOI: https://doi.org/10.1073/pnas.1814297116

Varga, T., Fisher, R.E., France, J.L., Haszpra, L., Jull, A.J.T., Lowry, D., Major, I., Molnár, M., Nisbet, E.G. and **László, E.** (2021) Identification of potential methane source regions in Europe using δ13C-CH4 measurements and trajectory modeling. *J. Geophys. Res. Atmospheres*, 126: e2020JD033963. DOI: https://doi.org/10.1029/2020JD033963

Wehr, R. and **Saleska, S.R.** (2017) The long-solved problem of the best-fit straight line: application to isotopic mixing lines. *Biogeosciences*, 14: 17–29. DOI: https://doi.org/10.5194/bg-14-17-2017

Whiticar, M.J. (1999) Carbon and hydrogen isotope systematics of bacterial formation and oxidation of methane. *Chem. Geol.*, 161: 291–314. DOI: https://doi.org/10.1016/S0009-2541(99)00092-3

York, D. (1966) Least-squares fitting of a straight line. *Can. J. Phys.*, 44(5): 1079–1086. DOI: https://doi.org/10.1139/p66-090

York, D., Evensen, N.M., Martínez, M.L. and **De Basabe Delgado, J.** (2004) Unified equations for the slope, intercept, and standard errors of the best straight line. *Am. J. Phys.*, 72(3): 367–375. DOI: https://doi.org/10.1119/1.1632486

Zazzeri, G., Lowry, D., Fisher, R.E., France, J.L., Lanoisellé, M. and **Nisbet, E.G.** (2015) Plume mapping and isotopic characterisation of anthropogenic methane sources. *Atmos. Environ.*, 110: 151–162. DOI: https://doi.org/10.1016/j.atmosenv.2015.03.029

Zobitz, J.M., Keener, J.P., Schnyder, H. and **Bowling, D.R.** (2006) Sensitivity analysis and quantification of uncertainty for isotopic mixing relationships in carbon cycle research. *Agric. For. Meteorol.*, 136: 56–75. DOI: https://doi.org/10.1016/j.agrformet.2006.01.003

TO CITE THIS ARTICLE:
Defratyka, S.M., France, J.L., Fisher, R.E., Lowry, D., Fernandez, J.M., Bakkaloglu, S., Yver-Kwok, C., Paris, J.-D., Bousquet, P., Arnold, T., Rennick, C., Helmore, J., Yarrow, N. and Nisbet, E.G. 2025. Evaluation of Data Processing Strategies for Methane Isotopic Signatures Determined During Near-Source Measurements. *Tellus B: Chemical and Physical Meteorology*, 77(1): 1–17. DOI: https://doi.org/10.16993/tellusb.1878

Submitted: 24 July 2024 **Accepted:** 16 January 2025 **Published:** 06 February 2025

Tellus B: Chemical and Physical Meteorology is a peer-reviewed open access journal published by Stockholm University Press.